IEICE TRANS. COMMUN., VOL.E95–B, NO.3 MARCH 2012

PAPER

Single Front-End MIMO Architecture with Parasitic Antenna Elements

Mitsuteru YOSHIDA[†a)], **Kei SAKAGUCHI**[†b)], *Members*, *and* **Kiyomichi ARAKI**[†c)], *Fellow*

SUMMARY In recent years, wireless communication technology has been studied intensively. In particular, MIMO which employs several transmit and receive antennas is a key technology for enhancing spectral efficiency. However, conventional MIMO architectures require some transceiver circuits for the sake of transmitting and receiving separate signals, which incurs the cost of one RF front-end per antenna. In addition to that, MIMO systems are assumed to be used in low spatial correlation environment between antennas. Since a short distance between each antenna causes high spatial correlation and coupling effect, it is difficult to miniaturize wireless terminals for mobile use. This paper shows a novel architecture which enables mobile terminals to be miniaturized and to work with a single RF front-end by means of adaptive analog beam-forming with parasitic antenna elements and antenna switching for spatial multiplexing. Furthermore, statistical analysis of the proposed architecture is also discussed in this paper.

key words: *single front-end architecture, parasitic antenna elements, MIMO, equal gain combining*

1. Introduction

Conventional MIMO architectures need a transceiver circuit for each antenna, which means that multiple antenna systems increase power consumption and size of RF front-end circuit. Hence, a single RF front-end architecture is an ideal one to overcome this problem. Some techniques realizing MIMO with a single RF front-end circuit have been proposed. One such technique is to use parasitic antenna elements. The elements are not supplied with power and only reflect incident radio waves [1]. The single RF front-end MIMO can be realized when the value of variable reactances connecting to parasitic antenna elements are controlled properly so as to generate orthogonal directivity patterns, because each orthogonal directivity pattern is spatially independent and can receive spatial distinct signals [2]. Another technique for realizing MIMO with a single RF front-end is antenna switching method based on sampling theorem for band-limited signal [3]. In [4], spatial multiplexing with phase state preserved can be realized using antenna switching. If the phase of signals is obtained in addition to its' amplitude, a diversity combining technique of multiple antenna systems can be operated effectively in digital signal processing (DSP) stages. However, both techniques decrease the SNR because these processes cause aliasing and interference effect from other channels against desired signals. In order to avoid undesired effects, the rotation speed of antenna directivity or the antenna switching rate must be higher than signal bandwidth. Furthermore, channel selection filters are needed in front of these processes [5]. The problem common to both methods is deterioration in quality of the SNR. Beam-forming techniques in digital or analog dimension are well known as the method to improve the SNR by steering a directivity to desired signals. Adaptive analog beam-forming systems using parasitic antenna elements are called ESPAR antenna systems [6]. Of course, ESPAR systems with a single RF front-end can also achieve spatial multiplexing [7]. In contrast, to the best of our knowledge, few papers discuss the compatibility between antenna switching and analog beam-forming. This paper proposes a novel single RF front-end MIMO architecture which takes advantage of not only antenna switching for spatial multiplexing but also adaptive analog beam-forming by parasitic antenna elements for compensating the switching penalty. Although the proposed architecture necessitates antenna switching frequency higher than signal bandwidth, the operating frequency of steering directivity by parasitic antenna elements can be reduced down to the fading rate known as Doppler spread that characterizes the time variation of the channel; therefore, while the change of beams within the symbol period expands the signal bandwidth, the effect in the proposed architecture is negligible because the directivity pattern to the direction of arrival wave by parasitic antenna elements has not been changed during the symbol time.

2. SNR Penalty on Antenna Switching for Spatial Multiplexing

In wireless communication system where signals' bandwidth is limited, the Sampling theorem states that signals have redundancy in time domain. The received RF signal, $s_m(t)$, at m-th antenna with spectrum, $S_m(f) = 0$ in $|f - f_c| > B/2$ where f_c is carrier frequency, can be recovered when the signal is sampled in a time period shorter than $1/B$, even though the SNR of switched signal deteriorates.

Now, consider the system which consists of M antennas in Fig. 1 where the band-limited RF signal impinges at each antenna and passed through a band pass filter (BPF) which is needed for anti-aliasing caused by switching operation at next stage, but not for selecting channels. Channel

Manuscript received April 18, 2011.
Manuscript revised August 17, 2011.

[†]The authors are with the Tokyo Institute of Technology, Tokyo, 152-8550 Japan.
a) E-mail: mitsuteru@mobile.ee.titech.ac.jp
b) E-mail: sakaguchi@mobile.ee.titech.ac.jp
c) E-mail: araki@mobile.ee.titech.ac.jp

DOI: 10.1587/transcom.E95.B.882

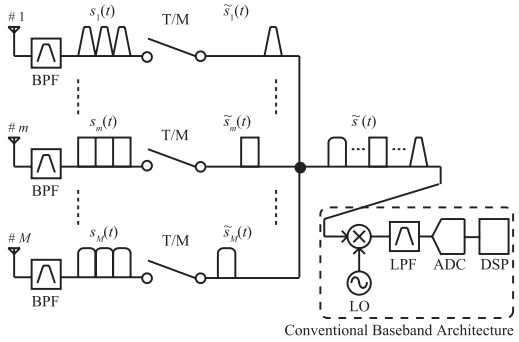

Fig. 1 Antenna switching operation.

selection is performed at the baseband by DSP. Then, the RF signal is sampled and holded during T/M time period.

The switched signal, $\tilde{s}_m(t)$, at m-th antenna is expressed as the product of $s_m(t)$ and $u_m(t)$ defined by Eq. (1) in the form of Fourier series.

$$\begin{aligned} u_m(t) &\triangleq \sum_{n=-\infty}^{\infty} \sqcap\left(\frac{M}{T}\left(t - \frac{m-1}{M}T - nT\right)\right) \\ &= \frac{1}{M}\sum_{n=-\infty}^{\infty} \frac{\sin(\pi n/M)}{\pi n/M} e^{j2\pi\frac{n}{T}\left(t-\frac{m-1}{M}T\right)}, \end{aligned} \tag{1}$$

where

$$\sqcap(x) = \begin{cases} 1 & \text{if } x \in \left[-\frac{1}{2}, \frac{1}{2}\right] \\ 0 & \text{if } x \notin \left[-\frac{1}{2}, \frac{1}{2}\right] \end{cases} \tag{2}$$

Then, the SNR of switched and sampled signal is derived as follows. Wiener-Khinchin theorem states that power spectrum density (PSD) is the Fourier transform of auto-correlation function. $\tilde{s}_m(t)$ has the auto-correlation function, $\tilde{A}_m(\tau)$, as Eq. (3) because $s_m(t)$ has the auto-correlation function, $A_m(\tau) = \mathcal{E}[s_m(t)s_m(t+\tau)]$, if $s_m(t)$ is wide sense stationary. Note that $\mathcal{E}[\cdot]$ denotes expectation operator.

$$\begin{aligned} \tilde{A}_m(\tau, t) &= \mathcal{E}[\tilde{s}_m(t)\tilde{s}_m(t+\tau)] \\ &= \frac{A_m(\tau)}{M^2}\sum_{n=-\infty}^{\infty} \frac{\sin^2(\pi n/M)}{(\pi n/M)^2} e^{-j2\pi\frac{n}{T}\tau} \end{aligned} \tag{3}$$

According to Wiener-Khinchin theorem, $\tilde{S}_m(f)$ is of the form shown in Eq. (4). Note that $\mathcal{F}[\cdot]$ denotes Fourier transform operator.

$$\begin{aligned} \tilde{S}_m(f) &= \mathcal{F}\left[\tilde{A}_m(\tau)\right] \\ &= \frac{1}{M^2}\sum_{n=-\infty}^{\infty} \frac{\sin^2(\pi n/M)}{(\pi n/M)^2} \\ &\quad \times \int_{-\infty}^{\infty} A_m(\tau) e^{-j2\pi\frac{n}{T}\tau} e^{-j2\pi f\tau} d\tau \\ &= \frac{1}{M^2}\sum_{n=-\infty}^{\infty} \frac{\sin^2(\pi n/M)}{(\pi n/M)^2} S_m\left(f + \frac{n}{T}\right) \end{aligned} \tag{4}$$

Furthermore, a PSD of switched white noise, $\tilde{N}(f)$, is

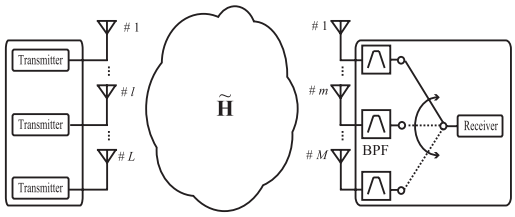

Fig. 2 Equivalent MIMO channel.

of the form in Eq. (5), provided that the white noise has a constant PSD, $N_0/2$, before switching. Note that $B_2(x)$ is the Bernoulli polynomial of second degree.

$$\begin{aligned} \tilde{N}(f) &= \frac{1}{M^2}\sum_{n=-\infty}^{\infty} \frac{\sin^2(\pi n/M)}{(\pi n/M)^2}\frac{N_0}{2} \\ &= \frac{1}{M^2}\left\{1 + \frac{M^2}{\pi^2}\sum_{n=1}^{\infty}\frac{1}{n^2} - M^2 B_2\left(\frac{1}{M}\right)\right\}\frac{N_0}{2} \\ &= \frac{1}{M}\frac{N_0}{2} \quad \therefore \tilde{N}(f) = \frac{N(f)}{M} \end{aligned} \tag{5}$$

Assuming that $s_m(t)$ is band-limited in $|f - f_c| \le B/2$ and switching period for m-th antenna, T, is shorter than $1/B$, then the switching operation does not cause aliasing. Therefore, the signal can be recovered according to the Sampling theorem. However, the SNR of switched signal through the BPF whose bandwidth equals B is deteriorated by $10\log M$ [dB] from Eq. (6) where γ is the average branch SNR before switching.

$$\frac{\int_{f_c-B/2}^{f_c+B/2}\tilde{S}_m(f)df}{\int_{f_c-B/2}^{f_c+B/2}\tilde{N}(f)df} = \frac{\int_{f_c-B/2}^{f_c+B/2}\frac{1}{M^2}S_m(f)df}{\int_{f_c-B/2}^{f_c+B/2}\frac{1}{M}N(f)df} = \frac{\gamma}{M} \tag{6}$$

From above discussion, equivalent MIMO channel in Fig. 2, $\tilde{\mathbf{H}}$, affected by switching operation is expressed as Eq. (7) where $\mathbf{H}$ and $\mathbf{h}_l$ are a conventional MIMO channel and a $M \times 1$ conventional channel vector respectively.

$$\tilde{\mathbf{H}} = \left[\frac{1}{\sqrt{M}}\mathbf{h}_1, \cdots, \frac{1}{\sqrt{M}}\mathbf{h}_l, \cdots, \frac{1}{\sqrt{M}}\mathbf{h}_L\right] = \frac{1}{\sqrt{M}}\mathbf{H} \tag{7}$$

3. Statistical Analysis of Parasitic Antenna Element System

In previous section, it has been shown that antenna switching architecture can realize spatial multiplexing at the expense of performance degradation as compared to conventional MIMO architecture, and the SNR penalty of switching process is evaluated theoretically. In order to overcome this penalty, we apply an adaptive beam-forming with parasitic antenna elements to our architecture. Parasitic antenna elements (PAEs) are connected not to the RF front-end but to the variable reactance. Re-radiation effect of these elements enable us to steer the directivity adaptively by changing the value of reactances. In the switching process for spatial multiplexing, the single RF front-end is connected to only one

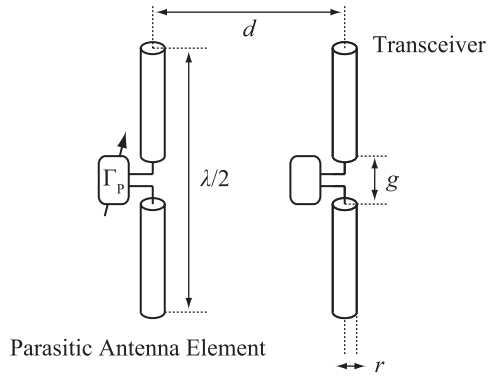

Fig. 3 Parasitic antenna element system.

antenna, whereas the other antennas are terminated in open or connected to dummy loads. At this, if these unconnected antennas are tapped to variable reactances and deployed as PAEs, the PAEs contribute to improve the SNR. This section shows that this proposed operation is sufficient for compensating the penalty of SNR and its average error probability is the same stochastic characteristic of Equal Gain Combining (EGC) in digital signal processing.

Now, consider a system which consists of one transmit antenna, one receive antenna and one PAE. Since PAE and usual antenna exchange the their roles as whether receive antenna or PAE periodically in antenna switching frequency, the state fixed in a period is equivalent to Fig. 3. Analysis of this system leads us to obtain statistical characteristics of the proposed architecture. First, let us define a scattering matrix of free space and a reflection coefficient of the reactance value connected to the PAE as $\mathbf{S}$ and Γ_{P} respectively. Then, a scattering matrix of free space including parasitic antenna elements, $\tilde{\mathbf{S}}$, is expressed by Eq. (9) [8].

$$\mathbf{S} \triangleq \begin{bmatrix} S_{\mathrm{TT}} & S_{\mathrm{TR}} & S_{\mathrm{TP}} \\ S_{\mathrm{RT}} & S_{\mathrm{RR}} & S_{\mathrm{RP}} \\ S_{\mathrm{PT}} & S_{\mathrm{PR}} & S_{\mathrm{PP}} \end{bmatrix} \tag{8}$$

$$\tilde{\mathbf{S}} \triangleq \begin{bmatrix} \tilde{S}_{\mathrm{TT}} & \tilde{S}_{\mathrm{TR}} \\ \tilde{S}_{\mathrm{RT}} & \tilde{S}_{\mathrm{RR}} \end{bmatrix} \Leftrightarrow \begin{cases} \tilde{S}_{\mathrm{TT}} = S_{\mathrm{TT}} + S_{\mathrm{TP}}(\Gamma_{\mathrm{P}}^{-1} - S_{\mathrm{PP}})^{-1} S_{\mathrm{PT}} \\ \tilde{S}_{\mathrm{TR}} = S_{\mathrm{TR}} + S_{\mathrm{TP}}(\Gamma_{\mathrm{P}}^{-1} - S_{\mathrm{PP}})^{-1} S_{\mathrm{PR}} \\ \tilde{S}_{\mathrm{RT}} = S_{\mathrm{RT}} + S_{\mathrm{RP}}(\Gamma_{\mathrm{P}}^{-1} - S_{\mathrm{PP}})^{-1} S_{\mathrm{PT}} \\ \tilde{S}_{\mathrm{RR}} = S_{\mathrm{RR}} + S_{\mathrm{RP}}(\Gamma_{\mathrm{P}}^{-1} - S_{\mathrm{PP}})^{-1} S_{\mathrm{PR}} \end{cases} \tag{9}$$

Therefore, the spectral efficiency in this model is formulated by Eq. (10) where γ is average branch SNR, provided $|\Gamma_{\mathrm{P}}| \leq 1$ holds: the PAE are passive.

$$\begin{aligned} C/B &= \mathcal{E}\left[\max_{|\Gamma_{\mathrm{P}}|\leq 1} \log\left(1+\gamma\left|\tilde{S}_{\mathrm{RT}}\right|^2\right)\right] \\ &= \mathcal{E}\left[\log\left(1+\gamma \max_{|\Gamma_{\mathrm{P}}|\leq 1}\left|\tilde{S}_{\mathrm{RT}}\right|^2\right)\right] \end{aligned} \tag{10}$$

From Eq. (10), maximization problem on the spectral efficiency results in another maximization problem on the channel gain, $\left|\tilde{S}_{\mathrm{RT}}\right|$, because a logarithm function is monotonically increasing.

If a random variable, W, is defined as the maximum value of the channel gain, W can be rewritten as Eq. (11) and optimal reflection coefficient of parasitic antenna element, $\Gamma_{\mathrm{P}}^{\mathrm{opt}}$, is determined uniquely and written as Eq. (12).

$$\begin{aligned} W &\triangleq \max_{|\Gamma_{\mathrm{P}}|\leq 1}\left|\tilde{S}_{\mathrm{RT}}\right| \\ &= \left|S_{\mathrm{RT}} + \frac{S_{\mathrm{PP}}^* S_{\mathrm{RP}} S_{\mathrm{PT}}}{1-|S_{\mathrm{PP}}|^2}\right| + \frac{|S_{\mathrm{RP}} S_{\mathrm{PT}}|}{1-|S_{\mathrm{PP}}|^2} \end{aligned} \tag{11}$$

$$\begin{aligned} \Gamma_{\mathrm{P}}^{\mathrm{opt}} &= \operatorname*{argmax}_{|\Gamma_{\mathrm{P}}|\leq 1} \log\left(1+\gamma\left|\tilde{S}_{\mathrm{RT}}\right|^2\right) = \operatorname*{argmax}_{|\Gamma_{\mathrm{P}}|\leq 1}\left|\tilde{S}_{\mathrm{RT}}\right| \\ &= \frac{\frac{S_{\mathrm{RP}}S_{\mathrm{PT}}S_{\mathrm{PP}}^*}{|S_{\mathrm{RP}}S_{\mathrm{PT}}|} + \frac{(1-|S_{\mathrm{PP}}|^2)S_{\mathrm{RT}}+S_{\mathrm{RP}}S_{\mathrm{PT}}S_{\mathrm{PP}}^*}{\left|(1-|S_{\mathrm{PP}}|^2)S_{\mathrm{RT}}+S_{\mathrm{RP}}S_{\mathrm{PT}}S_{\mathrm{PP}}^*\right|}}{\frac{S_{\mathrm{RP}}S_{\mathrm{PT}}}{|S_{\mathrm{RP}}S_{\mathrm{PT}}|} + \frac{(1-|S_{\mathrm{PP}}|^2)S_{\mathrm{RT}}S_{\mathrm{PP}}+S_{\mathrm{RP}}S_{\mathrm{PT}}|S_{\mathrm{PP}}|^2}{\left|(1-|S_{\mathrm{PP}}|^2)S_{\mathrm{RT}}+S_{\mathrm{RP}}S_{\mathrm{PT}}S_{\mathrm{PP}}^*\right|}} \end{aligned} \tag{12}$$

If S_{RT} and S_{PT} are correlated random variables and follow a complex Gaussian distribution, $\mathcal{CN}\left(0,\sigma_{\mathrm{S}}^2\right)$, X and Y which are defined by Eq. (13) are Rayleigh random variables correlated to each other.

$$\begin{cases} X \triangleq \left|S_{\mathrm{RT}} + \frac{S_{\mathrm{PP}}^* S_{\mathrm{RP}} S_{\mathrm{PT}}}{1-|S_{\mathrm{PP}}|^2}\right| \\ Y \triangleq \frac{|S_{\mathrm{RP}}S_{\mathrm{PT}}|}{1-|S_{\mathrm{PP}}|^2} \end{cases} \tag{13}$$

Let $p_W(w)$ be the probability density function (PDF) of W, and then it is of the form of Eq. (14) with joint PDF, $p_{X,Y}(x,y)$.

$$p_W(w) = \int_{-\infty}^{\infty}\int_{-\infty}^{\infty} \delta(w-x-y) p_{X,Y}(x,y)\,dxdy \tag{14}$$

Although it is difficult to obtain $p_W(w)$ in closed form [9], the average error probability of BPSK modulation in this model can be obtained because W consists of the sum of two Rayleigh random variables [10]. It means that this system has the same statistical characteristic as EGC which is a kind of diversity combiner.

When the random variables, $\mathbf{w} = [w_X, w_Y]^T$, follow a multivariate complex gaussian distribution, joint PDF, $p(\mathbf{w})$, is written as Eq. (15) subject to $\mathcal{E}[\mathbf{w}] = \mathbf{0}$ [11].

$$\begin{aligned} p(\mathbf{w}) &= \frac{1}{\pi^2 |\det \Psi|} \exp\left(-\mathbf{w}^\dagger \Psi^{-1} \mathbf{w}\right) \\ \Psi &= \mathcal{E}\left[\mathbf{w}\mathbf{w}^\dagger\right] \triangleq \begin{bmatrix} \sigma_X^2 & \sigma_X\sigma_Y\zeta \\ \sigma_X\sigma_Y\zeta^* & \sigma_Y^2 \end{bmatrix} \end{aligned} \tag{15}$$

The absolute value of random variables, $X = |w_X|$ and $Y = |w_Y|$, have the joint PDF, $p_{X,Y}(x,y)$, which is written as Eq. (16).

$$\begin{aligned} p_{X,Y}(x,y) &= \frac{4xy}{\sigma_X^2\sigma_Y^2\left(1-|\zeta|^2\right)} \\ &\quad \times \exp\left(-\frac{\sigma_Y^2 x^2 + \sigma_X^2 y^2}{\sigma_X^2\sigma_Y^2\left(1-|\zeta|^2\right)}\right) \\ &\quad \times I_0\left(\frac{2xy\,|\zeta|}{\sigma_X\sigma_Y\left(1-|\zeta|^2\right)}\right) \end{aligned} \tag{16}$$

Therefore, the characteristic function of this joint PDF, $\phi_W(\xi)$, is expressed by Eq. (17) where $\Gamma(x)$ is the gamma function and ${}_1F_1(a;b;x)$ is the Kummer's function of the first kind [12].

$$\phi_W(\xi) = \left(1-|\zeta|^2\right)\sum_{n=0}^{\infty}\left[\left(\frac{|\zeta|^n}{n!}\right)^2 L_{0,n}\left(\xi;|\zeta|^2;\sigma_X^2\right) \times L_{0,n}\left(\xi;|\zeta|^2;\sigma_Y^2\right)\right], \tag{17}$$

where

$$\begin{aligned} L_{0,n}\left(\xi;|\zeta|^2;\sigma^2\right) \triangleq\ & \Gamma(n+1) \\ & \times {}_1F_1\left(n+1;\frac{1}{2};-\frac{\sigma^2\left(1-|\zeta|^2\right)}{4}\xi^2\right) \\ & + j\xi\left[\sigma^2\left(1-|\zeta|^2\right)\right]^{\frac{1}{2}}\Gamma\left(n+\frac{3}{2}\right) \\ & \times {}_1F_1\left(n+\frac{3}{2};\frac{3}{2};-\frac{\sigma^2\left(1-|\zeta|^2\right)}{4}\xi^2\right) \end{aligned}$$

Since the statistical characteristic in this model does not depend on any modulation formats, for the simplicity in analysis, we assume that the transmitted signal, s, is modulated by BPSK. Then, the received signal, r, after coherent detection in PAE system is expressed by Eq. (18). Note that an additive noise, z, follows $\mathcal{CN}\left(0,\sigma_{\mathrm{N}}^2\right)$, and $\Re[\cdot]$ denotes the real part of a complex number.

$$r = (X+Y)s + \Re[z] = Ws + n_{\mathrm{I}} \tag{18}$$

Therefore, the average error probability, P_e, of BPSK modulation in coherent detection equals $P_r(0)$ because Eq. (19) holds where $P_r(r)$ is cumulative distribution function of received signal.

$$P_e = \begin{cases} \text{Probability in } r<0 \text{ where } s=1 \\ \text{Probability in } r>0 \text{ where } s=-1 \end{cases} \tag{19}$$

$\phi_{n_{\mathrm{I}}}(\xi)$ is the characteristic function of In-phase component of noise and is expressed by $\exp\left(-\frac{1}{2}\frac{\sigma_{\mathrm{N}}^2}{2}\xi^2\right)$. Provided that n_{I} is random variable independent of W and s, the characteristic function of r, $\phi_r(\xi)$, is the product of $\phi_W(\xi)$ and $\phi_{n_{\mathrm{I}}}(\xi)$ which are characteristic functions of W and n_{I} respectively. Therefore, $\phi_r(\xi)$ is written as Eq. (20).

$$\phi_r(\xi) = \left(1-|\zeta|^2\right)\sum_{n=0}^{\infty}\left[\left(\frac{|\zeta|^n}{n!}\right)^2 L_{0,n}\left(\xi;|\zeta|^2;\sigma_X^2\right) \times L_{0,n}\left(\xi;|\zeta|^2;\sigma_Y^2\right)\right] \times e^{-\frac{1}{4}\sigma_{\mathrm{N}}^2\xi^2} \tag{20}$$

According to Gil-Pelaez's inversion formula [13], cumulative distribution function and characteristic function have a relationship shown in Eq. (21). Note that $\Im[\cdot]$ denotes the imaginary part of a complex number.

$$P_r(0) = \frac{1}{2} - \frac{1}{\pi}\int_0^{\infty}\frac{\Im\left[\phi_r(\xi)\right]}{\xi}d\xi \tag{21}$$

Thus, the average error probability is obtained as Eq. (22) from Eq. (20) and Eq. (21). Note that ${}_2F_1(a,b;c;x)$ denotes the Gauss' hypergeometric function.

$$\begin{aligned} P_e = P_r(0) = \frac{1}{2} & - \frac{1-|\zeta|^2}{2}\sum_{n=0}^{\infty}\binom{2n}{n}\left(\frac{|\zeta|}{2}\right)^{2n} \\ & \times \sum_{k=0}^{n}\binom{n}{k}(-1)^k\frac{2n+1}{2k+1} \\ & \times \left[\left\{\frac{\sigma_Y^2}{\frac{\sigma_{\mathrm{N}}^2}{1-|\zeta|^2}+\sigma_X^2+\sigma_Y^2}\right\}^{k+\frac{1}{2}} \right. \\ & \times {}_2F_1\left(-n-\frac{1}{2},k+\frac{1}{2};\frac{1}{2};\frac{\sigma_X^2}{\frac{\sigma_{\mathrm{N}}^2}{1-|\zeta|^2}+\sigma_X^2+\sigma_Y^2}\right) \\ & + \left\{\frac{\sigma_X^2}{\frac{\sigma_{\mathrm{N}}^2}{1-|\zeta|^2}+\sigma_X^2+\sigma_Y^2}\right\}^{k+\frac{1}{2}} \\ & \left. \times {}_2F_1\left(-n-\frac{1}{2},k+\frac{1}{2};\frac{1}{2};\frac{\sigma_Y^2}{\frac{\sigma_{\mathrm{N}}^2}{1-|\zeta|^2}+\sigma_X^2+\sigma_Y^2}\right)\right] \end{aligned} \tag{22}$$

Given σ_X^2, σ_Y^2 and ζ, theoretical curves can be drawn. These parameters of the system now considered are summarized in Eq. (23) where a correlation coefficient, ρ, is defined as $\mathcal{E}\left[S_{\mathrm{RT}}S_{\mathrm{PT}}^*\right]/\sigma_{\mathrm{S}}^2$. Equation (23) shows that ρ is modified by S_{RP} and S_{PP}, ζ, therefore, indicates a modified correlation coefficient in this model.

$$\begin{cases} \sigma_X^2 = \left(1+\left|\frac{S_{\mathrm{PP}}^*S_{\mathrm{RP}}}{1-|S_{\mathrm{PP}}|^2}\right|^2+2\Re\left[\rho\frac{S_{\mathrm{PP}}S_{\mathrm{RP}}^*}{1-|S_{\mathrm{PP}}|^2}\right]\right)\sigma_{\mathrm{S}}^2 \\ \sigma_Y^2 = \left(\frac{|S_{\mathrm{RP}}|}{1-|S_{\mathrm{PP}}|^2}\right)^2\sigma_{\mathrm{S}}^2 \\ \zeta = \frac{\rho\frac{S_{\mathrm{RP}}^*}{1-|S_{\mathrm{PP}}|^2}+\frac{S_{\mathrm{PP}}^*|S_{\mathrm{RP}}|^2}{\left(1-|S_{\mathrm{PP}}|^2\right)^2}}{\sigma_X\sigma_Y}\sigma_{\mathrm{S}}^2 \end{cases} \tag{23}$$

The squared absolute value of ρ coincides with the envelope correlation [14] or the power correlation [15] in our assumption. $|\rho|^2$ is often given by Jakes' model [16] or Blanch's model [17]. Since the Jakes' model assumes that no mutual coupling between two dipoles exists and the directivity is omni-directional, the Blanch's model is more appropriate to the PAE case that is a narrow spacing case where the lower correlation coefficient is observed [18]. Figures 4 and 5 show that the results of Monte Carlo simulation are consistent with theoretical curves where average branch SNR, γ, is expressed by $\sigma_{\mathrm{S}}^2/\sigma_{\mathrm{N}}^2$ and ρ is given by Eq. (24) as Blanch's model for symmetric antenna structure. Furthermore, theoretical curves of two branch Maximum Ratio Combining (MRC) given by Eq. (25) and two branch EGC are also plotted in Figs. 4 and 5 for comparison.

$$|\rho|^2 = \frac{\left|2\Re\left[S_{\mathrm{PP}}^*S_{\mathrm{RP}}\right]\right|^2}{\left(1-\left(|S_{\mathrm{PP}}|^2+|S_{\mathrm{RP}}|^2\right)\right)^2} \tag{24}$$

$$P_e = \frac{1}{2} - \frac{1}{4|\rho|}\left\{(1+|\rho|)\sqrt{\frac{\gamma(1+|\rho|)}{\gamma(1+|\rho|)+1}} - (1-|\rho|)\sqrt{\frac{\gamma(1-|\rho|)}{\gamma(1-|\rho|)+1}}\right\} \quad (25)$$

Table 1 shows the antenna structure parameter and Table 2 shows the S parameter of this model calculated by Ansoft HFSS in 3.0 GHz, assuming that antennas consist of perfect electric conductor. Equation (22) states that optimal adaptive beam-forming in this system, in spite of only one receiver, has the same stochastic characteristic as two branch EGC. In particular, Fig. 5 shows that performance of PAE system in $d = \lambda/8$ is almost the same as that of two branch MRC. From these results it is believed that the adaptive beam-forming using the PAE is equivalent to the technique co-phasing the signals on each pseudo-branch, w_X and w_Y, as if two antennas are deployed and the EGC technique is applied to the signals. Since the performance of EGC is quite close to that of MRC which achieves full diversity order, typically exhibiting less than 1 dB of power penalty [19], the PAE operation with high mutual coupling can increase the SNR by about 2 to 3 dB in $d = \lambda/8$.

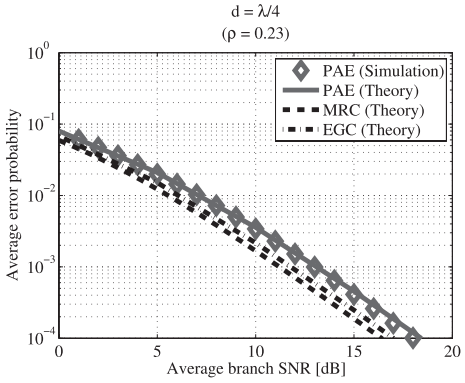

Fig. 4 Average error probability of PAE system where $d = \lambda/4$.

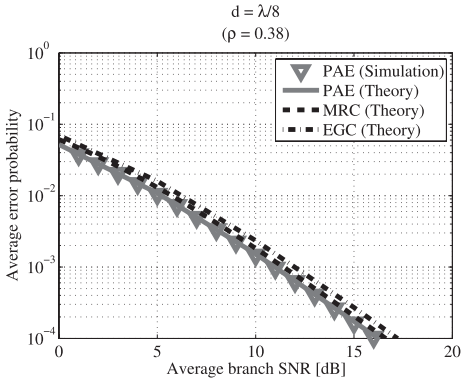

Fig. 5 Average error probability of PAE system where $d = \lambda/8$.

Table 1 Antenna structure parameters in Fig. 3.

λ[m]	g[m]	r[m]
0.100	$\lambda/1000$	$\lambda/1000$

Table 2 S parameters in Fig. 3.

	S_{RP}	S_{PP}
$d = \lambda/4$	$-0.00888 - j0.258$	$0.444 + j0.281$
$d = \lambda/8$	$0.218 - j0.378$	$0.330 + j0.442$

4. Performance Evaluation of Proposed Architecture

In previous sections, it has been shown that PAE operation can improve the error probability. In the case of $M = 2$ and $d = \lambda/8$, in particular, Sect. 2 shows that the switching effect decreases the SNR by 3 dB and Sect. 3 shows that PAE operation increases the SNR by 3 dB. Therefore, notwithstanding a single RF front-end, performance of the transceiver equipped with both switching architecture and PAE operation seems to be the same as that of conventional one. Figure 6 shows our proposed architecture in MIMO case. In this section, performance of the proposed architecture is evaluated by computer simulation in terms of spectral efficiency subject to 2×2 MIMO as shown in Fig. 7. In the simulation, conventional channel matrix is generated by Kronecker model [20] where the receiving correlation is only considered and given by Blanch's model.

In this simulation model, equivalent MIMO channel is written as Eq. (26) and the spectral efficiency is calculated by Eq. (27). Note that ${}^t[\cdot]$ denotes transpose operator and $\langle\cdot,\cdot\rangle$ denotes inner product operator.

$$\tilde{\mathbf{H}} = \frac{1}{\sqrt{2}}\begin{bmatrix}\tilde{S}_{RT_1}(\Gamma_1) & \tilde{S}_{RT_2}(\Gamma_1)\\ \tilde{S}_{PT_1}(\Gamma_2) & \tilde{S}_{PT_2}(\Gamma_2)\end{bmatrix} \triangleq \frac{1}{\sqrt{2}}\begin{bmatrix}{}^t\tilde{\mathbf{h}}_1(\Gamma_1)\\ {}^t\tilde{\mathbf{h}}_2(\Gamma_2)\end{bmatrix} \quad (26)$$

$$C/B = \max_{|\Gamma_1|,|\Gamma_2|\le 1} \log\det\left(\mathbf{I} + \gamma\tilde{\mathbf{H}}\tilde{\mathbf{H}}^\dagger\right) = \log \max_{|\Gamma_1|,|\Gamma_2|\le 1}\left[1 + \frac{\gamma}{2}\left(\left|\tilde{\mathbf{h}}_1\right|^2 + \left|\tilde{\mathbf{h}}_2\right|^2\right)\right.$$

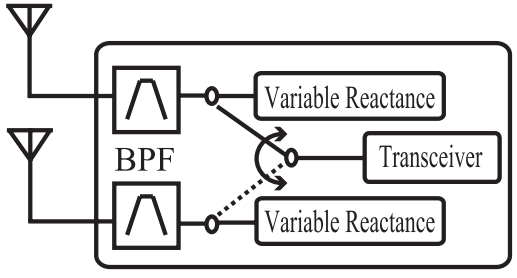

Fig. 6 SF-MIMO w/ PAE: Single Front-end MIMO with Parasitic Antenna Element.

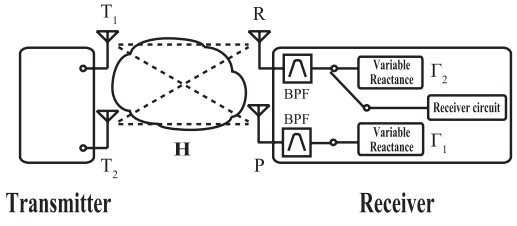

Fig. 7 Simulation model.

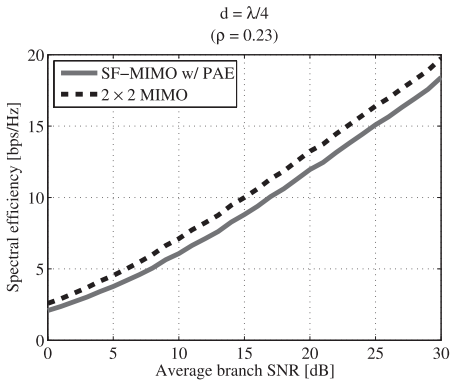

Fig. 8 Spectral efficiency of proposed architecture where $d = \lambda/4$.

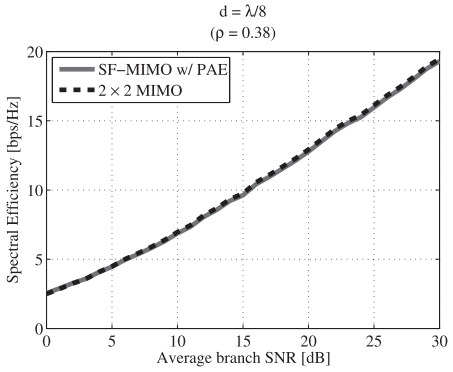

Fig. 9 Spectral efficiency of proposed architecture where $d = \lambda/8$.

$$+\left(\frac{\gamma}{2}\right)^2\left(\left|\tilde{\mathbf{h}}_1\right|^2\left|\tilde{\mathbf{h}}_2\right|^2-\left|\left\langle\tilde{\mathbf{h}}_1,\tilde{\mathbf{h}}_2\right\rangle\right|^2\right)\Bigg] \tag{27}$$

According to Eq. (27), this maximization problem is a combinatorial optimization because there is the term $\left\langle\tilde{\mathbf{h}}_1,\tilde{\mathbf{h}}_2\right\rangle$ in this equation. A full search algorithm with 1 degree step size is used in order to find the optimal reflection coefficients, Γ_1^{opt} and Γ_2^{opt}. Results of this simulation are shown in Figs. 8 and 9.

While Fig. 8 shows that performance of the proposed architecture is worse than that of conventional one because of insufficient improvement by PAE, Fig. 9 shows that performance of the proposed architecture is improved by about 2 to 3 dB as expected and then the switching penalty for spatial multiplexing is compensated. In addition to that, in a case with higher mutual coupling and spatial correlation compared with $d = \lambda/8$, we obtained a result that the spectral efficiency of the proposed architecture remains but that of the conventional architecture deteriorates. These results confirm that performance of the proposed architecture is tolerant to high spatial correlation environment while the conventional MIMO architecture suffers performance degradation from high spatial correlation environment.

5. Conclusion

A novel architecture that realizes single RF front-end by antenna switching for spatial multiplexing and improvement of SNR by adaptive beam-forming was proposed. Furthermore, statistical analysis of the antenna switching system with a parasitic antenna element was discussed theoretically. It was confirmed that the distribution of improved channel by our proposed architecture is identical to that of the output from equal gain combiner. This paper also showed that the results of computer simulation in MIMO case give the performance of proposed architecture with $d = \lambda/8$, which is the same as that of conventional one. As a result, this scheme provides compact transceivers.

References

[1] R. Dinger, "Reactively steered adaptive array using microstrip patch elements at 4 GHz," IEEE Trans. Antennas Propag., vol.32, no.8, pp.848–856, Aug. 1984.
[2] R. Bains and R.R. Muller, "Using parasitic elements for implementing the rotating antenna for MIMO receivers," IEEE Trans. Wirel. Commun., vol.7, no.11, pp.4522–4533, Nov. 2008.
[3] F. Adachi, T. Hattori, K. Hirade, and T. Kamata, "A periodic switching diversity technique for a digital FM land mobile radio," IEEE Trans. Veh. Technol., vol.27, no.4, pp.211–219, Nov. 1978.
[4] J.D. Fredrick, Y. Wang, and T. Itoh, "A smart antenna receiver array using a single RF channel and digital beamforming," IEEE Trans. Microw. Theory Tech., vol.50, no.12, Dec. 2002.
[5] M. Taromaru and H. Aino, "Fast periodic antenna switching for diversity and smart antenna: On SNR property and spurious response," IEEE Antennas and Propagation Society International Symposium 2006, pp.4553–4556, July 2006.
[6] T. Ohira and K. Gyoda, "Electronically steerable passive array radiator antennas for low-cost analog adaptive beamforming," IEEE International Conference on Phased Array Systems and Technology, pp.101–104, 2000.
[7] A. Kalis, A. Kanatas, and C. Papadias, "A novel approach to MIMO transmission using a single RF front end," IEEE J. Sel. Areas Commun., vol.26, no.6, pp.972–980, Aug. 2008.
[8] N. Honma, K. Nishimori, R. Kudo, Y. Takatori, T. Hiraguri, and M. Mizoguchi, "A stochastic approach to design MIMO antenna with parasitic elements based on propagation characteristics," IEICE Trans. Commun., vol.E93-B, no.10, pp.2578–2585, Oct. 2010.
[9] D. Brennan, "Linear diversity combining techniques," Proc. IEEE, vol.91, no.2, pp.331–356, Feb. 2003.
[10] R. Mallik, M. Win, and J. Winters, "Performance of dual-diversity predetection EGC in correlated rayleigh fading with unequal branch snrs," IEEE Trans. Commun., vol.50, no.7, pp.1041–1044, July 2002.
[11] K.S. Miller, "Complex Gaussian processes," SIAM Review, vol.11, no.4, pp.544–567, Oct. 1969.
[12] D. Middleton, An Introduction to Statistical Communication Theory, McGraw-Hill, New York, 1960.
[13] J. Gil-Pelaez, "Note on the inversion theorem," Biometrika, vol.38, no.3-4, pp.481–482, 1951.
[14] R.G. Vaughan and J.B. Andersen, "Antenna diversity in mobile communications," IEEE Trans. Veh. Technol., vol.36, no.4, pp.149–172, Nov. 1987.
[15] J.R. Mendes and M.D. Yacob, "Power correlation coefficient of a general fading model," SBMO/IEEE MTT-S International Conference on Microwave and Optoelectronics, pp.497–502, July 2005.
[16] W.C. Jakes and D.C. Cox, eds., Microwave Mobile Communications, Wiley-IEEE Press, 1994.
[17] S. Blanch, J. Romeu, and I. Corbella, "Exact representation of antenna system diversity performance from input parameter description," Electron. Lett., vol.39, no.9, pp.705–707, May 2003.
[18] Y. Yamada, K. Kagoshima, and K. Tsunekawa, "Diversity antennas for base and mobile stations in land mobile communication sys-

tems," IEICE Trans. Commun., vol.E74-B, no.10, pp.3202–3209, Oct. 1991.
[19] A. Goldsmith, Wireless Communications, Cambridge University Press, 2005.
[20] J.P. Kermoal, L. Schumacher, K.I. Pedersen, P.E. Mogensen, and F. Frederiksen, "A stochastic MIMO radio channel model with experimental validation," IEEE J. Sel. Areas Commun., vol.20, no.6, pp.1211–1226, Aug. 2002.

Mitsuteru Yoshida was born in 1985. He received the B.E. and the M.E. degree in electrical and electronic engineering from Tokyo Institute of Technology, Japan, in 2008 and 2010. In 2010, he joined the NTT Network Innovation Laboratories, Nippon Telegraph and Telephone Corporation (NTT). This work had done when he was a student at Tokyo Institute of Technology.

Kei Sakaguchi was born in 1973. He received the B.E. degree in electrical and computer engineering from Nagoya Institute of Technology, Japan, in 1996, and the M.E. degree in information processing from Tokyo Institute of Technology, in 1998, and the Ph.D. degree in electrical and electronic engineering from Tokyo Institute of Technology, in 2006. From 2000 to 2007, he was an Assistant Professor at Tokyo Institute of Technology. Since 2008, he has been an Associate Professor at the same university. He received the Young Engineer Awards from IEICE and IEEE AP-S Japan chapter in 2001 and 2002 respectively, the Outstanding Paper Awards from SDR Forum and IEICE in 2004 and 2005 respectively, and the Tutorial Paper Award from IEICE communication society in 2006. His current interests are MIMO propagation measurements, MIMO communication systems, and software/cognitive radio. He is a member of IEEE.

Kiyomichi Araki was born in 1949. He received the B.S. degree in electrical engineering from Saitama University, Japan, in 1971, and the M.S. and the Ph.D. degrees in physical electronics both from Tokyo Institute of Technology, in 1973 and 1978, respectively. From 1973 to 1975, and from 1978 to 1985, he was a Research Associate at Tokyo Institute of Technology. From 1985 to 1995, he was an Associate Professor at Saitama University. In 1979–1980 and 1993–1994, he was a visiting research scholar at University of Texas, Austin and University of Illinois, Urbana, respectively. Since 1995, he has been a Professor at Tokyo Institute of Technology. His research interests are information security, coding theory, communication theory, ferrite devices, RF circuit theory, electromagnetic theory, and microwave circuits, etc. He is a member of IEEE and Information Processing Society of Japan. He is currently serving as a chair of Japan Chapter of IEEE MTT-S and a chair of Japan National committee of APMC.